Heliyon 9 (2023) e18212

Contents lists available at ScienceDirect

Heliyon

journal homepage: www.cell.com/heliyon

Research article

Dynamic modeling and data fitting of climatic and environmental factors and people's behavior factors on hand, foot, and mouth disease (HFMD) in Shanghai, China

Changlei Tan [a,b], Shuang Li [c], Yong Li [a,*], Zhihang Peng [d,*]

[a] School of Information and Mathematics, Yangtze University, Jingzhou, 434023, Hubei, PR China
[b] Information Engineering College, Hunan Applied Technology University, Changde, 415100, Hunan, PR China
[c] College of Mathematics and Information Science, Henan Normal University, Xinxiang, 453000, Henan, PR China
[d] School of Public Health, Nanjing Medical University, Nanjing, 211166, Jiangsu, PR China

ARTICLE INFO

Keywords:
Hand, foot, and mouth disease
Temperature
Relative humidity
School opening and closing
Distributed lag nonlinear model
Basic reproduction number

ABSTRACT

Background: Hand, foot, and mouth disease (HFMD) appear to be a multi-wave outbreak with unknown mechanisms. We investigate the effects of climatic and environmental factors and changes in people's behavior factors that may be caused by external factors: temperature, relative humidity, and school opening and closing.

Methods: Distributed lag nonlinear model (DLNM) and dynamic model are used to research multi-wave outbreaks of HFMD. Climatic and environmental factors impact on transmission rate $\beta(t)$ is modeled through DLNM and then substituted into this relationship to establish the dynamic model with reported case data to test for validity.

Results: Relative risk (RR) of HFMD infection increases with increasing temperature. The RR of infection first increases and then decreases with the increase of relative humidity. For the model fitting HFMD dynamic, time average basic reproduction number [R_0] of Stage I (without vaccine) and Stage II (with EV71 vaccine) are 1.9362 and 1.5478, respectively. Temperature has the highest explanatory power, followed by school opening and closing, and relative humidity.

Conclusion: We obtain three conclusions about the prevention and control of HFMD. 1) According to the temperature, relative humidity and school start time, the outbreak peak of HFMD should be warned and targeted prevention and control measures should be taken. 2) Reduce high indoor temperature when more than 31.5 °C, and increase low relative humidity when less than 77.5% by opening the window for ventilation, adding houseplants, using air conditioners and humidifiers, reducing the incidence of HFMD and the number of infections. 3) The risk of HFMD transmission during winter vacations is higher than during summer vacations. It is necessary to strengthen the publicity of HFMD prevention knowledge before winter vacations and strengthen the disinfection control measures during winter vacations in children's hospitals, school classrooms, and other places where children gather to reduce the frequency of staff turnover during winter vacations.

* Corresponding authors.
E-mail addresses: yongli@yangtzeu.edu.cn (Y. Li), zhihangpeng@njmu.edu.cn (Z. Peng).

https://doi.org/10.1016/j.heliyon.2023.e18212
Received 9 December 2022; Received in revised form 8 July 2023; Accepted 11 July 2023

Available online 24 July 2023

1. Introduction

Hand, foot, and mouth disease (HFMD) is caused by enteroviruses, which are RNA viruses. The main pathogenic Enterovirus serotypes of HFMD included Coxsackievirus (CV) A type 4 – 7, 9, 10, 16 and B type 1 – 3, 5, some serotypes of Echovirus and enterovirus 71 (Enterovirus A71, EV71), among which Coxsackievirus-A16 and EV71 are the most common, and most severe and fatal cases are caused by EVA71 [1–4]. The EV71 vaccine prevents HFMD caused by the dominant strain of HFMD, EV71, and will significantly reduce the number of severe and fatal cases of HFMD. The Chinese Center for Disease Control and Prevention reports that the EV71 vaccine is the only one currently available. Coxsackievirus A6 (CV6) and A10 (CV10) have caused epidemics in China, Japan, Thailand, and France since 2015 [5–8]. HFMD spreads through feces, saliva, nasal secretions, fluid from blisters or scabs [9–11]. Currently, transmission hot spots are mainly found in schools, daycare centers, and other large concentrations of infants and children [12–14]. The common symptoms include fever, sores in the mouth, and rashes with blisters on the hands, feet, and buttocks [5,10]. HFMD mainly occurs in children under five years old, and the incubation period is 2–10 days [10,15]. HFMD mainly affects children under five years of age, but adults who are in high contact with children are the main group infected in other age groups. The majority of time, HFMD is mild and self-limiting, without specific medication, and many people get better within 7 to 10 days [16]. However, some infected people may have no symptoms or severe complications, including aseptic meningitis, encephalitis, acute flaccid paralysis, and pulmonary edema, all can be life-threatening [10,17,18]. More than a million HFMD reported cases annually in China, resulting in sporadic challenges for infectious disease prevention and public health [19,20].

Understanding the process of multi-wave outbreaks of HFMD is critical to public health so that policy makers can anticipate outbreaks before they occur. Current understanding of HFMD epidemiology indicates that it has a certain periodicity, which may be caused by various climatic and environmental factors such as temperature and relative humidity [11,21]. HFMD outbreaks often occur in multiple waves in China every year, reaching the peak in spring and autumn, which may be related to schools opening and closing. At present, numerous studies on the dynamics of HFMD have focused on discussing isolation [22–25], vaccines [6,25–28], treatment [28–31], simulations of real cases [23,24,32–36] and contaminated environments [25,33,34,37], and study the transmission of HFMD qualitatively and quantitatively. However, the existing dynamic models do not describe the basic cause of the multi-wave outbreak of HFMD. Therefore, it is very important to study the outbreak of HFMD from the epidemiological perspective for the prevention and control of HFMD. By referring to other existing results [38–41], we find that the outbreak of seasonal diseases is closely related to a variety of climate, environmental factors and human behavior habits. So, the purpose of this study is to explore the mechanism of multiple outbreaks of HFMD with the help of dynamic models and the method of controlling HFMD based on environmental factors. Compared with general statistical models, dynamic models can better evolve past outbreak patterns and predict future outbreaks. There are very few studies on the effects of temperature, relative humidity, and school vacations on HFMD with the help of dynamic models.

Different from the existing periodic incidence to describe the outbreak of HFMD [22,23,26,34], we decide to consider the actual climate, environmental data, the specific time of school opening and closing, and select appropriate functions to simulate the influence of the above factors on the outbreak of HFMD. This consideration will more realistically reflect the influence of climate and environment on the spread of HFMD. The function is chosen to describe temperature, humidity, and other climatic and environmental factors is often essential for disease transmission. Certainly, Distributed lag nonlinear model (DLNM) method in statistics can be used. It can consider the potential linear, nonlinear, and delayed effects between two or more variables. The DLNM proposed by Gasparini et al. [42,43] is widely applied in disease research [44–48]. It is derived from classical statistical models that study the linear and lag effects between variables, such as generalized linear models (GLM), generalized additive models (GAM), and distributed lag linear models (DLM).

The results of dynamic studies on existing HFMD are insufficient. We focus on the effects of temperature, relative humidity, and school opening and closing on the transmission of HFMD. The structure of our paper is here: In the second section, we propose the HFMD epidemic dynamic models to consider three factors on $\beta(t)$. In the third section, we obtain the specific forms of $\beta(t)$ by DLNM. Then, we use the models to fit Shanghai HFMD cases from 2012 to 2019, select the best model, estimate the optimal model parameters and calculate the time average basic reproduction number $[R_0]$. In the fourth section, DLNM results, $[R_0]$, and sensitivity of parameters are analyzed in detail. The discussion and conclusion are in the last two sections.

2. Model

2.1. Study area and data

Shanghai (30°40′ ~31°53′N, 120°52′ ~122°12′E) is one of the four direct-administered municipalities of China in Fig. 1, with an area of 6340.5 km^2 and a resident population of 24.88 million in 2020 [49]. Shanghai has a subtropical monsoon climate, mild and humid, with an annual average temperature of 17.8 °C and annual average relative humidity of 75% in 2020.

Since 2008, Ministry of Health of the People's Republic of China declared HFMD as a Category C infectious disease (Infectious Disease Surveillance and Management) and provided the diagnosis basis for HFMD Control and Prevention Guidelines [50]. Chinese Center for Disease Control and Prevention (CCDC) collects data of HFMD patients every month. CCDC has published the report data of HFMD in all provinces (except Hong Kong, Macao and Taiwan). Among them, Shanghai Municipal Health Commission has published the monthly case data of HFMD in the study area of Shanghai in the form of a web page [51]. The data are shown in Fig. 4 (blue line), with the multi-wave outbreak. Since the EV71 vaccine was launched in November 2016, we divided the total time into two stages, namely stage I (without vaccine) and stage II (with vaccine).

Fig. 1. The location of Shanghai city in China.

The monthly temperature data are collected from the main meteorological index entries of each month in the Shanghai Statistical Yearbook 2021 released by the Shanghai Bureau of Statistics [52]. Our paper uses the monthly mean temperature data, which is calculated by adding the average temperature of each day of the whole month and dividing by the number of days in the month. The monthly relative humidity data are collected from the Shanghai section of the average relative humidity of major cities in China in 2021 China Statistical Yearbook [53]. Average relative humidity refers to the ratio of the actual water pressure in the air to the saturated water pressure at the prevailing temperature, and is calculated in the same way as the air temperature. The monthly temperature relative humidity is shown in Fig. 2a.

Air pollution data [54] are collected from 19 widely distributed monitoring stations in Shanghai, all updating their data online every hour. Our research's air pollutant data are averages of 24-hour monitoring concentrations at 19 stations published on the monitoring website.

2.2. Epidemic model

In order to simplify the problem and focus on the study itself, we make the following assumptions before modeling:

1) The population is assumed to be homogeneous, so differences in age, gender and so on are ignored.
2) The effect of enterovirus of different genotypes in different seasons is ignored.
3) According to data released by the Data-center of China Public Health Science [55] in 2018, 92.76% of children are under the age of 5, and 99.36% are under 14 in China, so we ignore other age groups.
4) Our study is based on monthly data, so we ignore the influence of the minor holidays and Lunar New Year (7 days) on the spread of HFMD in Shanghai.

According to epidemiological characteristics, the total population $N(t)$ is divided into six subgroups based on their infectious status: susceptible $S(t)$, exposed but not yet infectious $E(t)$, infectious with symptoms $I(t)$, infectious but not yet symptomatic (asymptomatic infectious) $I_e(t)$, infectious and hospitalized or quarantined or other ways be isolated from $H(t)$, and recovered $R(t)$ at time t.

The transmission rate $\beta(t)$ considers temperature, relative humidity, and school opening and closing, as follows:

1) Temperature and relative humidity are crucial factors in the transmission of human infectious diseases by influencing the biological activity, transmission, and proliferation of pathogens [56–58].
2) School is opening and closing to characterize children's behavioral changes. It influences the incidence of HFMD by influencing the contact between susceptible groups of children. The specific time is obtained from the school calendar [59] of the Education Bureau. The winter vacations vary from mid-January to late February, and the summer vacations are from July to August.

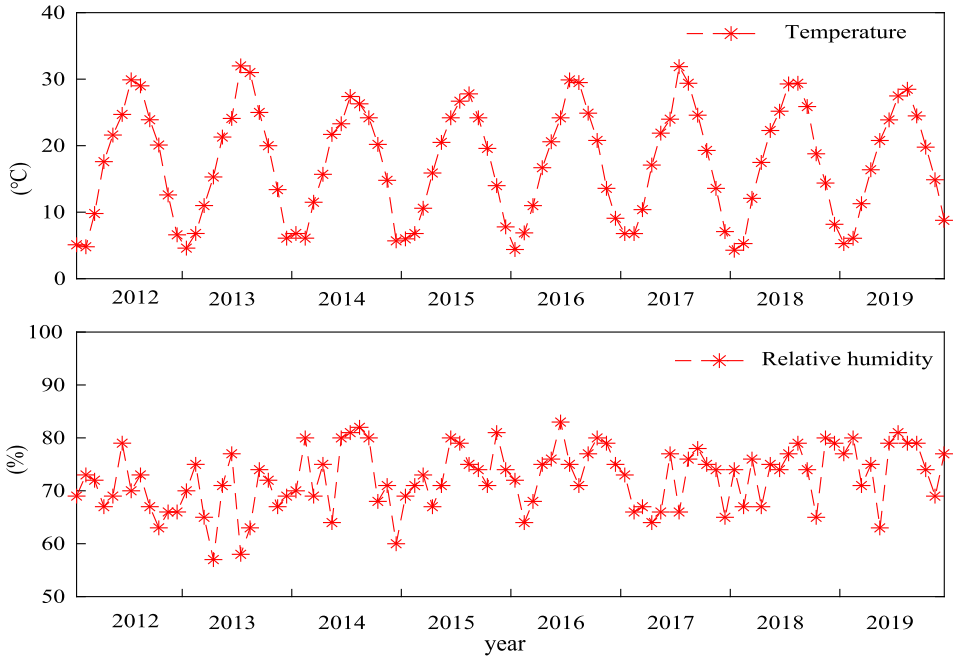

(a) Temperature and relative humidity in Shanghai from January 2012 to December 2019.

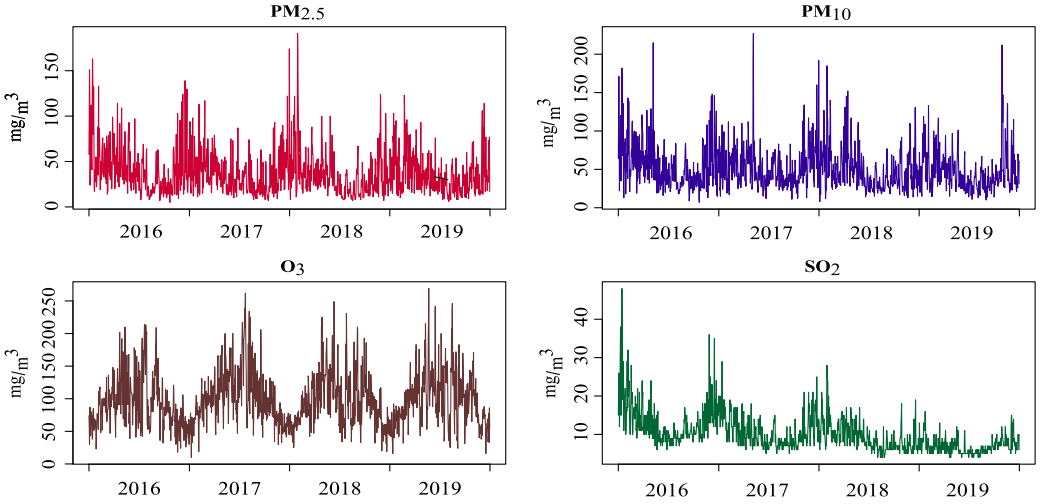

(b) Periodic phenomena of four air pollutants in Shanghai, China, from January 2016 to December 2019.

Fig. 2. Data of Temperature, relative humidity, PM2.5, PM10, SO_2, and O_3.

Table 1
Parameter definition of HFMD model equations (1).

Parameter	Definition
Λ	Recruitment rate
ρ	Proportion of susceptible vaccinated with EV71 vaccine
r	Infection reducing factor
η	Remove rate from $R(t)$ to $S(t)$
μ	Natural mortality rate
σ	Rate of progression to be infected
p	Proportion of infected people with symptoms
q	Proportion of infected people hospitalized or isolated vaccine
d	Mortality rate caused by HFMD
$\gamma_1, \gamma_2, \gamma_3$	Recovery rate of $I(t), I_e(t)$ and $R(t)$, respectively

Phase III clinical trials have shown that the EV71 vaccine protects significantly against EV71-induced HFMD, up to 90% [60]. Based on this, we believe that people vaccinated with EV71 are entirely immune to EV71-induced HFMD; Obviously, these people are at risk for HFMD caused by other viruses, as shown in function $f(t)$. The vaccine is also considered in the $f(t)$. Since there was no vaccine in Shanghai before November 2016, the proportion of susceptible population is set at 1. After the vaccine is used locally in Shanghai, the number of susceptible people consists of two parts. Suppose the proportion of the population receiving this vaccine is ρ, so the proportion of the unvaccinated population is $1-\rho$. The susceptible population is $(1-\rho)S(t)$. In addition, after the development of the EV71 vaccine, because EV71 vaccine does not have cross protection against other viruses caused by HFMD, so people who have been vaccinated still have a certain possibility of contracting the disease. However, these people are less likely to be infected with HFMD, so the infection reduction factor r is used in our model. Finally, after November 2016, the susceptible population is $f(t)S(t)$, of which $f(t)=1-\rho+r\rho$ in equation (2).

The differential equations for the HFMD model are as follows, and the parameters are defined in Table 1.

$$\begin{cases} \frac{dS}{dt} = \Lambda - \frac{\beta(t)f(t)S(I+I_e)}{N} + \eta R - \mu S, \\ \frac{dE}{dt} = \frac{\beta(t)f(t)S(I+I_e)}{N} - \sigma E - \mu E, \\ \frac{dI}{dt} = \sigma p E - \gamma_1 I - \mu I, \\ \frac{dI_e}{dt} = \sigma(1-p)E - \gamma_2 I_e - \mu I_e, \\ \frac{dH}{dt} = \gamma_1 q I - \gamma_3 H - d H - \mu H, \\ \frac{dR}{dt} = \gamma_1(1-q)I + \gamma_2 I_e + \gamma_3 H - \eta R - \mu R, \end{cases} \tag{1}$$

which

$$f(t) = \begin{cases} 1, & t \le November\ 2016, \\ 1-\rho+r\rho, & t > November\ 2016. \end{cases} \tag{2}$$

2.3. Time average basic reproduction number $[R_0]$

The basic reproduction number R_0 indicates the outbreak's severity, which is a threshold parameter. R_0 represents the number of people that an initial patient can spread during an infection period. For a threshold system, the disease will persist when $R_0 > 1$, the disease will die out when $R_0 < 1$ [61]. The equations (1) with initial condition $(S(0), E(0), I(0), I_e(0), H(0), R(0)) \in R_+^6$, according to P. Van den Driessche [61], we can compute the time average basic reproduction number $[R_0]$ in equation (3) (See Appendix A for calculations):

$$[R_0] = \begin{cases} \frac{\overline{\beta}\sigma(p\gamma_2+(1-p)\gamma_1+\mu)}{(\sigma+\mu)(\gamma_1+\mu)(\gamma_2+\mu)}, & t \le November\ 2016 \\ \frac{\overline{\beta}\sigma(p\gamma_2+(1-p)\gamma_1+\mu)(1-\rho+r\rho)}{(\sigma+\mu)(\gamma_1+\mu)(\gamma_2+\mu)}, & t > November\ 2016 \end{cases} \tag{3}$$

and

$$\overline{\beta} = \frac{1}{T}\int_0^T \beta(t)dt, \tag{4}$$

which T shows the epidemic period of HFMD in equation (4).

3. Methods

The distributed lag nonlinear model (DLNM) and dynamic model equations (1) are used in this paper. The relationship between temperature, relative humidity, and HFMD is obtained by DLNM. Then, above connections are used to construct the dynamic model equations (1) of transmission rate $\beta(t)$ to study the epidemic of HFMD.

3.1. Distributed lag nonlinear model (DLNM)

DLNM is a flexible framework for studying the nonlinear relationship between single or multiple variables and response variables by cross basis [42,43].

According to the existing research results, we find that temperature and humidity are extremely important for the incidence of HFMD [62–64]. To explore the relationship between temperature and relative humidity on HFMD simultaneously, we establish a DLNM model by cross-basis function $cb()$ based on some model [65,66]. Air pollutants are thought to affect HFMD in some studies [66–69]. Therefore, they are included in the model to obtain a more accurate relationship. Finally, our model is in equations (5) and (6), and the modeling steps are as follows:

$$\begin{aligned} \log[\mu_t] = {} & \alpha + cb(temp, df_1, lag, df_2) + cb(rh, df_3, lag, df_4) \\ & + \sum ns(X_i) + ns(time, df_5) + factor(weekday) + factor(holiday) \end{aligned} \tag{5}$$

and

$$\sum ns(X_i) = ns(\text{PM2.5}, df_6) + ns(SO_2, df_7) + ns(O_3, df_8), i = 1, 2, 3 \tag{6}$$

Step 1. Establish the nonlinear part of the model: Establish two cross basis of temperature and relative humidity by [11,65,66,70]. Y_t is the number of reported cases on day t, μ_t means the expectation of Y_t, $E(Y_t) = \mu_t$, α denotes the intercept. $temp$ for temperature, rh for relative humidity, and cb denote the cross-basis function used to estimate the relationship between temperature, relative humidity, and the incidence of HFMD. The $weekday$ is an indicator variable representing the day of the week. The $holiday$ represents a dichotomous variable that indicates whether day t is on vacation.

Step 2. Establish the linear part of the model: $ns()$ denotes a natural cubic spline function for the air pollution variable X_i. The long-term trends and seasonality are controlled by the variable $time$, the $factor()$ denotes the indicator variables. Spline knots are defined in equal space, and the lag knots are also defined on the equal log scale by default.

Step 3. Determine the variables of X_i: Previous studies have shown that sulfur dioxide (SO_2), ozone (O_3), particulate matter with an aerodynamic diameter of 2.5 microns or less (PM2.5), and particulate matter with an aerodynamic diameter of 10 microns or less (PM10), can potentially increase HFMD risk [66–69]. Therefore, we include the above four air pollutants in the analysis. Then, we check the correlation of temperature, relative humidity, and air pollutants. The examination results are shown in Figure S1 of the Supplementary material. The conclusion is that PM2.5 and PM10 correlation coefficient is 0.85. To avoid collinearity, we eventually include only PM2.5, SO_2, and O_3 in $ns(X_i)$ at equation (6), and use PM10 in Step 5. to test for robustness.

Step 4. Determine the parameter value: the maximum lag day is set to 14 days due to the incubation period and refers to similar studies [57,71,72], which aim to estimate the overall cumulative effect. The Akaike Information Criterion determines the degree of freedom (df) for each variable for quasi-Poisson (Q-AIC) [73]. For a 14-day lag, df ranges from 3 to 5 to represent complex lags [72]. df_1, df_2, df_3, df_4 are set as 5, 5, 4, and 5, respectively. Besides, df_5 for time with 8 degrees of freedom per year [70,72]. The natural cubic spline controls PM2.5, SO_2, and O_3 with 4, 4, and 4 degrees of freedom, respectively.

Step 5. Sensitivity analysis is carried out to verify the robustness of the model. Four sensitivity analyses are performed in the feasible interval [62]: (a) change PM2.5 to PM10. (b) Change the df of temperature is 4 to 6. (c) Change the df of relative humidity is 4 to 6. and (d) Change the df of long-term trends and seasonality is 7 to 9 per year. The results show no significant change, indicating Step 1. to 4. are reasonable and our DLNM is robust in Supplementary material.

Fig. 2a shows the meteorological factors, and Fig. 2b shows the air pollution. Periodicity is observed for PM2.5, PM10, and O_3. The concentration of SO_2 shows a downward trend, but seasonality is observed. Daily air pollution data come from the Shanghai Municipal Bureau of Ecology and Environment [54]. Other daily data required by DLNM are interpolated randomly from monthly temperature, monthly relative humidity and monthly cases using the bootstrap method [74,75]. Modeling and analysis in this section are done using the R packages “spline” and “dlnm”.

3.2. Parameter estimation and data fitting for epidemic model

On the basis of the biological significance of the parameters and according to the transmission characteristics of HFMD in Shanghai, we set the upper and lower bounds for each parameter as follows:

1) According to The 6th Population Census in 2010, the number of children aged 0-14 in Shanghai is 1985634 [76], so $S(0) = 2 \times 10^7$. Initially, 1046 cases were reported, setting $H(0)$ to range from 0 to 2000. Let the upper band of $E(0), I(0), I_e(0), R(0)$ be $10^6, 10^4, 10^4, 10^4$.
2) From 2012 to 2019, shanghai has an average of 1.12×10^5 newborns [77] per year, with 9333 per month, taking $\Lambda = 9000$.
3) Due to the lack of adequate case data for laboratory etiological diagnosis and classification, the infection reduction factor r is set to 0 to 1.
4) The annual mortality proportion of 3.95 per 10000 people [78], with 3.29×10^{-5} per month, so $d = 3.29 \times 10^{-5}$.
5) The duration of the loss of immunity is set as one month to three years, so η is set as 1/36 to 1.
6) As most HFMD patients clear up on their own within 7 to 10 days [16], the course of the disease $\gamma_1, \gamma_2, \gamma_3$ is considered to be $1/(10/30) = 3$ to $1/(7/30) = 4.2875$.
7) The incubation period usually ranges from 2 to 10 days [15] and is translated into months, so σ is set to $1/(10/30)$ to $1/(2/30)$, namely 3 to 15.
8) The hesitation period for patients to choose medical treatment is considered as 1 day to 10 days, 1/30 to 10/30 months, thus k is set as 3 to 30.
9) Both ρ, p, and q represent proportions whose ranges we cannot specify, so they are set from 0 to 1.
10) Assume that the person’s natural mortality follows a uniform distribution. The registered population in Shanghai accounts for 60% approximately, with a life expectancy of 83.67 years [49]. Moreover, the floating population accounts for 40% approximately, and the life expectancy is 77.3 years [79]. Therefore, the natural mortality rate of humans can be calculated as $\mu = 1/(83.66 \times 60\% + 77.3 \times 40\%) \times 12) = 0.00103$.

Table 2
The value, range, and sources of parameters, initial conditions, and $[R_0]$ in the model (I).

Parameter	Value	Range	Source	Parameter	Value	Range	Source
$E(0)$	2.270×10^5	$[0,10^6]$	Estimate	a_1	0.0248	$[0,1]$	Estimate
$I(0)$	4.285×10^2	$[0,10^4]$	Estimate	a_2	0.7885	$[0,100]$	Estimate
$I_e(0)$	8.654×10^3	$[0,10^4]$	Estimate	b	0.8934	$[0,1]$	Estimate
$R(0)$	3.764×10^3	$[0,10^4]$	Estimate	δ_1	0.0018	$[0,1]$	Estimate
$H(0)$	1.588×10^3	$[0,2\times10^3]$	Estimate	δ_2	0.1386	$[0,1]$	Estimate
β_0	7.1726	$[0.1,10]$	Estimate	σ	6.6122	$[3,15]$	Estimate
r	0.5136	$[0,1]$	Estimate	η	0.4127	$[0.0278,1]$	Estimate
ρ	0.4124	$[0,1]$	Estimate	$S(0)$	2×10^7	–	Fix
p	0.3340	$[0,1]$	Estimate	Λ	9000	–	Fix
q	0.0151	$[0,1]$	Estimate	μ	0.0010	–	Fix
γ_1	3.6232	$[3,4.2875]$	Estimate	d	3.29×10^{-5}	–	Fix
γ_2	3.1263	$[3,4.2875]$	Estimate	$[R_0]\ (stageI)$	1.9362	–	Calculate
γ_3	3.5192	$[3,4.2875]$	Estimate	$[R_0]\ (stageII)$	1.5478	–	Calculate

We estimate 15 parameters and 5 initial values in the above four models by calculating the sum of chi-square values [80–82] as in equation (7), respectively. We choose the particle swarm optimization algorithm [83–85] in the global optimization toolbox of MATLAB software. The algorithm is an evolutionary algorithm to help find the global optimal parameters.

$$J=\sum_{i=1}^{96}\frac{(H(t_i)-\hat{H}(t_i))^2}{\hat{H}(t_i)}, \tag{7}$$

where the study lasts 96 months from 2012 to 2019, $H(t_i)$ $(i=1,2,...,96)$ represents the number of reported cases each month and $\hat{H}(t_i)$ represents the estimated number of cases each month.

3.3. Model selection criteria for epidemic model

To test which biological hypothesis are more consistent with HFMD infection in Shanghai, we need to employ model selection methods to evaluate different models. Standard model selection criteria include the Akaike information criterion (AIC) [86] in equation (8), which compares models from the perspective of information entropy. Bayesian information criterion (BIC) [87] in equation (9), compares models from the decision theory perspective. The consistent AIC (CAIC) [88] in equation (10) imposes an additional penalty for complex models compared to the BIC. In large samples, the Hannan-Quinn criterion (HQC) [89] in equation (11) imposes a smaller penalty on complex models than BIC. Smaller values of these criteria indicate a better, more parsimonious submodel. *RMSE* for the root mean square error. Under a likelihood framework, these criteria can be written as:

$$AIC=-2log(L)+2k, \tag{8}$$

$$BIC=-2log(L)+k\ log(n), \tag{9}$$

$$CAIC=BIC+k, \tag{10}$$

$$HQC=-2\ log(L)+2k\ log(log(n)). \tag{11}$$

L is the likelihood function, k is the number of parameters, and n is the sample size. The models and corresponding information criteria values are shown in Supplementary material. Then, the $\beta(t)$ and parameters value of the model (I) are shown in Supplementary material and Table 2, respectively.

3.4. Sensitivity method for epidemic model

Sensitivity analysis is used to identify the degree of correlation between input parameters and output parameters. The sensitivity analysis essentially assesses the relative change of R_0 as the model parameters change. And in general, the basic reproduction number R_0 directly describes the spread of the disease. At present, the Latin hypercube sampling (LHS) method and partial rank correlation coefficients (PRCC) are generally combined to analyze the sensitivity of each parameter to R_0. Use this way to determine which parameters change have the larger effect on R_0.

In this paper, we use LHS method to obtain the sample matrix LHS matrix, and calculate the PRCC of R_0 to analyze the sensitivity of each parameter to R_0. Here, we assume that PRCC values are significant when the significance level is less than 0.01. The details are as follows. First we set the sample size to X. The probability density function of each parameter is divided into X equal probability $(1/X)$ intervals by Latin hypercube sampling method. We randomly select a value from each interval, so that each parameter generates X groups of values, and then randomly mixes X groups of different parameter values to calculate the values of R_0, namely the distribution of R_0. Through this distribution, the sensitivity of parameters to R_0 can be obtained, which provides a basis for subsequent research.

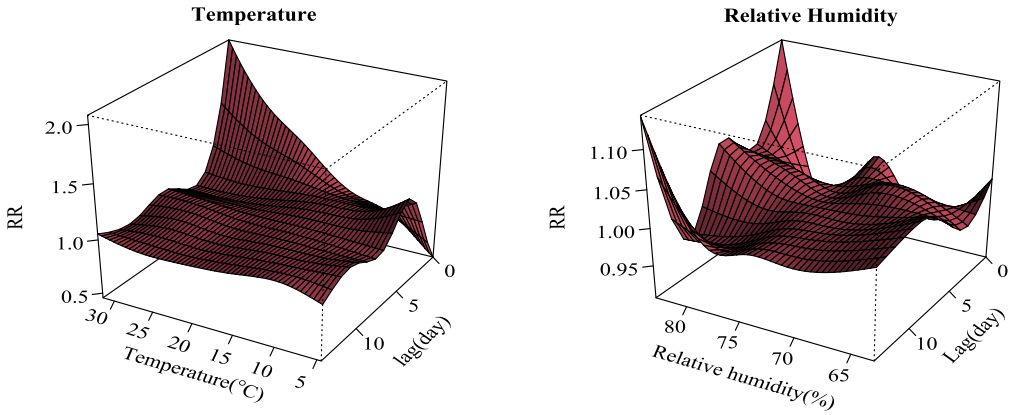

(a) The lag-response curves to temperature and relative humidity.

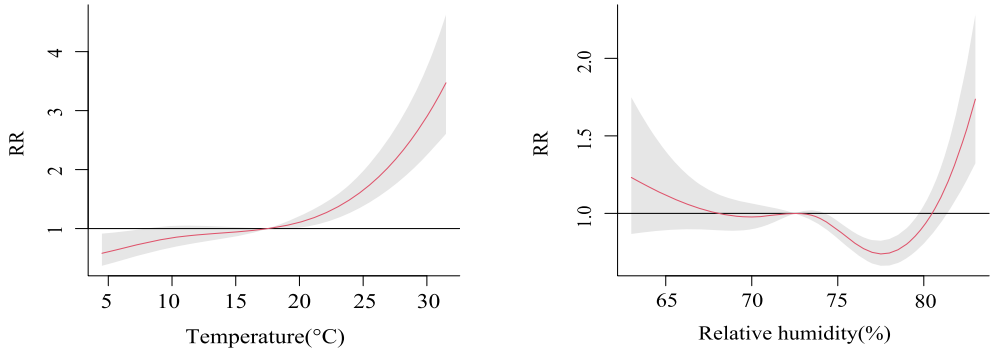

(b) Cumulative effects of temperature and relative humidity on HFMD incidence

Fig. 3. The relationship between temperature and relative humidity and HFMD cases by DLNM.

4. Result

4.1. Time-varying transmission rate $\beta(t)$

We use three-dimensional (3D) plots to visualize the relationship between HFMD cases and their delayed response to temperature and relative humidity in Fig. 3a. Fig. 3b shows the cumulative effect of temperature and relative humidity on infection's relative risk (RR), using their median values (17.5 °C, 72.5%) as the reference. The temperature-relative risk (RR) of the infection curve shows an exponential function, and the peak occurred at 31.5 °C with a relative risk (RR) of infection is 3.47 (95%CI: 2.61–4.62). The relative humidity-RR curve shows a U shape in favor of low humidity, and the lowest value occurred at 77.5% with a RR of 0.74 (95%CI: 0.66–0.82). According to the above figures, we used the exponential function to describe the relationship between temperature and the incidence of HFMD and the quadratic function to describe the relationship between relative humidity and the incidence of HFMD. Then, the relationship between school opening and closing and the incidence of HFMD is described by piecewise functions, consistent with other similar studies [40,41].

The above relationship between the incidence of HFMD and temperature and relative humidity obtained by DLNM, as an important result, has been considered in the $\beta(t)$ function of the key parameter of the epidemic model equations (1). The $\beta(t)$ has the form shown in equation (12), β_0 is the baseline transmission rate. $T(t)$ and $rh(t)$ in equation (13) are the temperature and relative humidity in month t, respectively. The a_1 and a_2 represent the strength of response to temperature and relative humidity, T and rh represent the average temperature and average relative humidity, respectively. δ_1 and δ_2 in equation (14) are the changes in transmission rates during summer and winter vacations relative to school opening, respectively.

$$\beta(t) = \beta_0 f_T(t) f_H(t) f_S(t), \tag{12}$$

which

$$f_T(t) = e^{a_1(T(t)-T)}, \quad f_H(t) = a_2(rh(t) - rh)^2 + b, \tag{13}$$

$$f_S(t)=\begin{cases}1-\delta_1, & t\in \text{winter vacation (January)},\\ 1-\delta_2, & t\in \text{summer vacation (July, August)},\\ 1, & t\in \text{other months every year};\ \delta_1,\delta_2\in[0,1].\end{cases} \tag{14}$$

4.2. Comparison of three multi-wave outbreak factors

$\beta(t)$ defines 4 scenarios since we can choose to turn off one of the three factors to study the effect of that factor in the epidemic model. Then, we focus on the following the model (I) $\beta(t)=\beta_0 f_T(t)f_H(t)f_S(t)$, and three "submodels": (i) only temperature and relative humidity, $\beta(t)=\beta_0 f_T(t)f_H(t)$, (ii) only temperature and school opening and closing, $\beta(t)=\beta_0 f_T(t)f_S(t)$, and (iii) only relative humidity and school opening and closing, $\beta(t)=\beta_0 f_H(t)f_S(t)$. Through these three submodels, we can compare the importance of these three factors.

The fitting results of the four models are shown in Fig. 4a-4d. At Stage I and Stage II, fitted cases (red) are consistent with reported cases (blue), which could explain the multi-wave outbreak of HFMD.

In the Supplementary material, model (I) has the smallest (best) selection criteria, indicating that model (I) has the best fitting effect. It is best to consider model (I) three factors. Therefore, we conclude that temperature, relative humidity, and school opening or closing play essential roles in HFMD multi-wave outbreaks. Our subsequent discussion will focus on model (I). Then, relative to model (I), submodel (iii) does not consider temperature and has the worst (maximum) selection criteria. The fitting effect is the worst ignoring the temperature factor. We conclude that temperature has the highest explanatory power for the multi-wave outbreak of HFMD. Based on similar comparisons, the explanation degree of HFMD multi-wave outbreak was temperature, school opening and closing, and relative humidity.

4.3. Comparative analysis of $[R_0]$

The smaller the R_0 in the epidemic model, the better for disease control. Our epidemic model incorporates actual temperature, relative humidity, and school data into the transmission rate $\beta(t)$, not a periodic model. $\beta(t)$ is averaged and substituted into R_0 to get $[R_0]$.

The estimated $[R_0]$ of the two stages are shown in Table 2, which are 1.9362 and 1.5478 respectively. First, we can see from the results that $[R_0]$ in the stage II is lower than that in the stage I, which indicates that the vaccine has an inhibitory effect on the transmission of HFMD. Secondly, the values of the basic reproduction number in both stages are greater than 1, indicating that the disease would persist. In other words, the vaccine alone cannot completely eliminate HFMD.

4.4. Parameter sensitivity analysis

We obtain the optimal epidemic model parameters in Table 2, and all parameters have biological significance. We calculated the sensitivity of $[R_0]$ to verify the effectiveness of the HFMD control strategy. All parameters in equations (3) and (4) of $[R_0]$ are used as input values, and the value of $[R_0]$ is used as output values and assuming that all input parameters are uniformly distributed. The sensitivity is compared with the relative change of $[R_0]$ as the model parameters change, is shown in Fig. 6. The larger the absolute value of PRCC of the parameter, the more sensitive the corresponding parameter. Therefore, we can draw a conclusion. In stage II, β and r has a positive effect on $[R_0]$; On the contrary, ρ, γ_1, and γ_2 have negative effects on $[R_0]$. And the most sensitive parameters are β, followed by the ρ, r, γ_1, and γ_2, respectively. Other parameters have no obvious influence. It has the potential to provide guiding information for HFMD prevention and control strategies.

In Fig. 3b, we observe that the relative risk (RR) of infection of HFMD is in the same trend as temperature, and the relative risk of infection increases with increasing temperature. The RR peaks at 31.5 °C. Then, we observe that the relative risk of infection of HFMD is different from that of relative humidity in trend. The relative risk of infection first increases and then decreases with the increase of relative humidity, reaching the lowest humidity at 77.5%. Therefore, to reduce the HFMD infection, we should avoid the temperature reaching the peak of 31.5 °C and increase the relative humidity to the lowest humidity at 77.5%. Combining with Fig. 3a, temperature and relative humidity play vital roles in the spread of HFMD with delaying and nonlinear effects. Extreme high temperature and extreme relative humidity increase the risk. Besides, low temperatures and middle relative humidity may reduce the incidence of HFMD.

5. Discussion

5.1. Basic reproduction number

As can be seen from the results of the basic reproduction number, we can find that the vaccine has a positive effect on curbing the spread of HFMD, but it cannot eliminate it. Therefore, in order to better control HFMD on the basis of vaccines, we still need more prevention and control measures. Many previous studies have combined dynamic models with real data to estimate the basic reproduction number of HFMD in China, ranging from 1.0414 to 1.7420 [23,24,32–35]. Our estimates are consistent with these results. But our estimated $[R_0]$ are slightly larger than the R_0 of these results. The reason could be that the risk of disease epidemics may be overestimated or underestimated by calculating the time average basic reproduction number $[R_0]$ [90–92]. And also some studies show that the time average reproduction number may not be as accurate as the basic reproduction number [22,23,34].

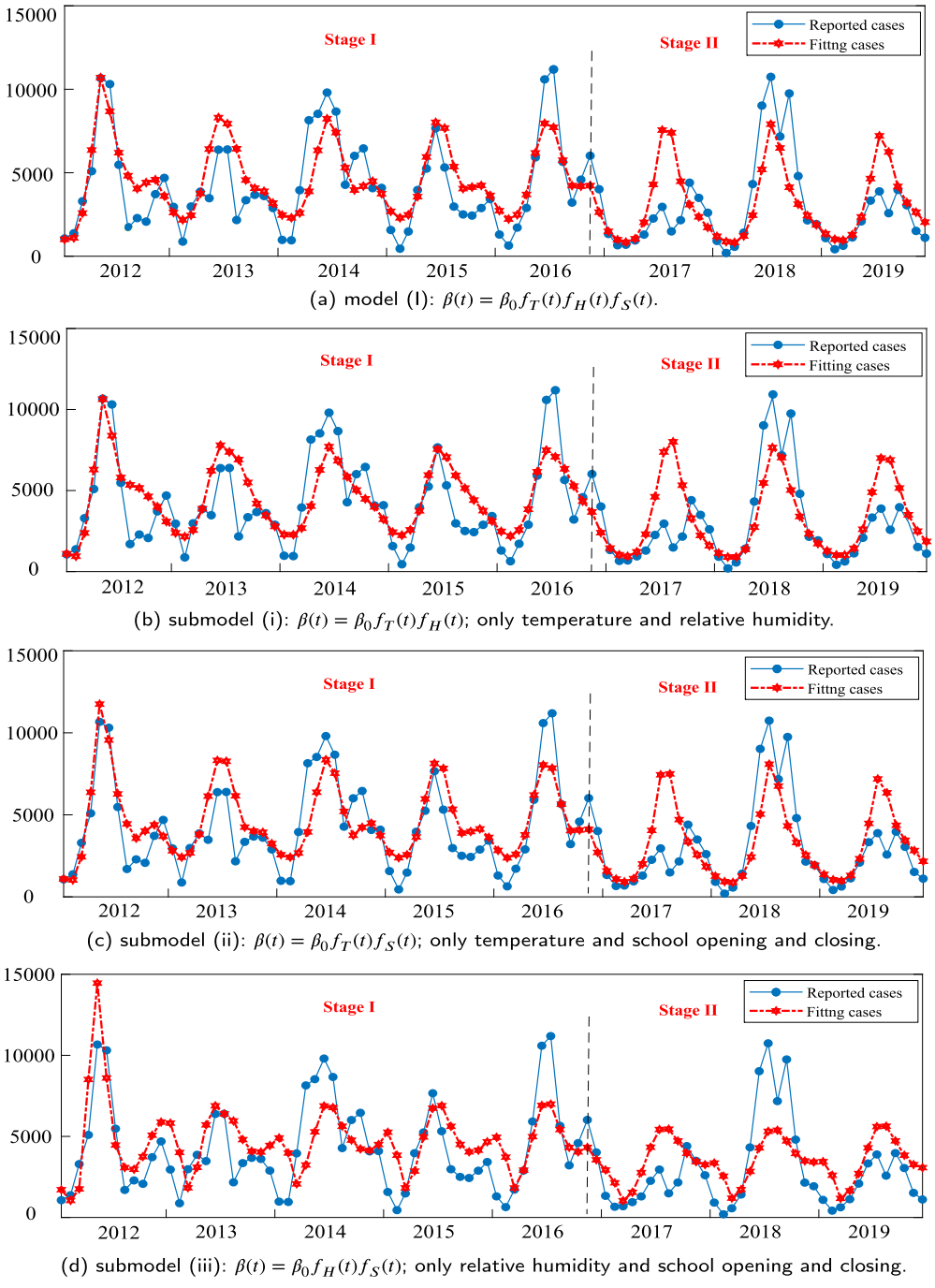

Fig. 4. Fitting the model (I) and its three submodels to reported cases of HFMD.

5.2. Estimated parameters

We also notice other estimated parameters in Table 2. $\delta_1 < \delta_2$, it indicates that the risk of infection during winter vacation is higher than that in summer vacation. According to the result and consideration of the actual situation, we think that the potential reason may be that winter vacation includes the Lunar New Year which greatly increases the frequency of people's exposure. In addition, cold weather may increase exposure by keeping people indoors. So it is necessary to strengthen the publicity of HFMD prevention knowledge before winter vacations and strengthen the disinfection control measures during winter vacations. The ρ is 0.41243, indicating about 41.2% of the population in Shanghai is vaccinated. Using climate and environment data and estimated parameters, we plot $f_T(t), f_H(t), f_S(t)$ and $\beta(t)$ in Fig. 5. We observe that $\beta(t)$ is almost periodic, which indicates that it is reasonable

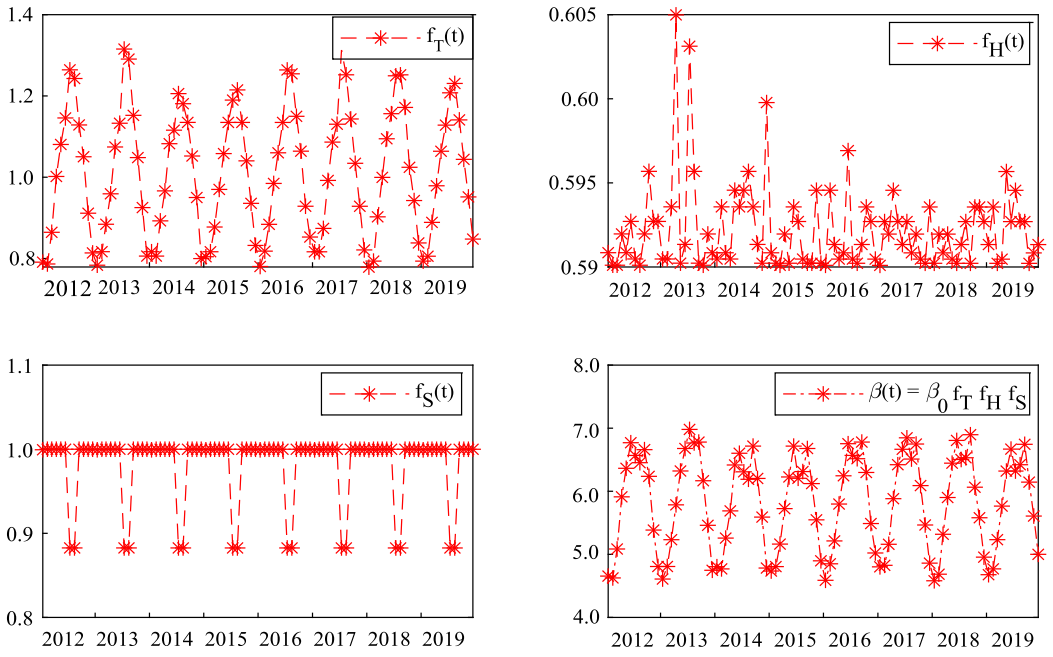

Fig. 5. The temperature function $f_T(t)$, relative humidity function $f_H(t)$, school opening and closing function $f_S(t)$, and transmission rate function $\beta(t)$ in the model (I).

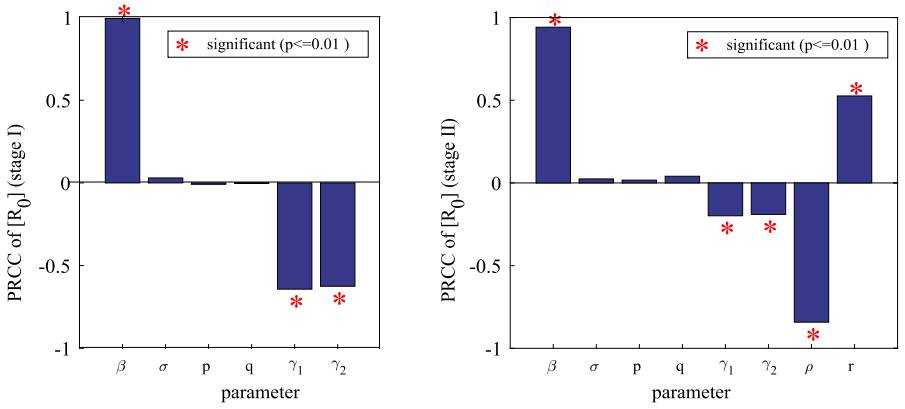

Fig. 6. The values of PRCC on the outcome of $[R_0]$. All parameter values are derived from Table 2 in the model (I).

to consider temperature, relative humidity, and school opening and closing to construct the periodicity transmission rate, which is consistent with other studies [22,23,34].

5.3. Three multi-wave outbreak factors

Our finding indicates that climatic and environmental factors indeed affect several domains of HFMD transmission. We obtain an exponential relationship for the temperature and incidence of HFMD in Shanghai, which is similar to the DLNM study of HFMD [72] in China from 2009 to 2014. And He et al. also use exponential functions [40,41] to describe the association between temperature and influenza incidence. Few DLNM studies of HFMD obtained the inverted U or M relationship [62,65], etc. For the relative humidity and incidence of HFMD in Shanghai, we obtain a quadratic function relationship, which is similar to the results of the DLNM study of HFMD conducted in Wuhan, China, from 2013 to 2017 [62]. Then, We agree with Zhao et al. that the association between temperature and HFMD varies across China [65] and that the impact of future climate change on HFMD incidence will vary, as these studies [63–65,72,93].

5.4. Applicability of models and methods

The study area in our paper is Shanghai which has a subtropical monsoon climate controlled alternately by tropical Marine air masses and polar continental air masses. Our study may be applicable to regions with climates (temperature, relative humidity)

similar to Shanghai we studied. Take Wuhan for example, Wuhan and Shanghai are similar in geography and climate. Shanghai is between 30°40′ and 31°53′ north latitude, while Wuhan is between 29°58′ and 31°22′ north latitude. The two cities have close latitude. Both cities belong to the Subtropical Monsoon Climate, which is controlled alternately by the tropical Marine air mass and the polar continental air mass. Therefore, the study of HFMD in Shanghai may provide a reference for the study of HFMD in Wuhan.

5.5. Research limitations

Our study has some limitations that could be improved and researches that can be done in the future.

We will consider age and gender in the HFMD model in the future when detailed data is available. With no data on reported HFMD cases daily. Shanghai's health and statistics authorities have released only monthly data on HFMD, with no data related to age or gender. After obtaining detailed data, more valuable results and conclusions can be obtained according to age and gender.

Winter vacations and Lunar New Year may impact the infection of HFMD. However, since we are looking at monthly data, we ignore the influence of the minor holidays and the Luner New Year. Therefore, we don't conduct in-depth research on it in the paper. We will study it in detail when sufficient data is available.

The registered population and floating population in shanghai are similar in size and reporting methods, but the number of reported cases differs significantly. Therefore, in the following article, we will divide the registered and floating populations into two groups, which belong to multiple groups problems in epidemiological dynamics and will be valuable.

Based on the 2015 report [5–8], Coxsackievirus A6 (CV6) and A10 (CV10) have caused epidemics in China. It is reasonable to guess that the dominant strains in Shanghai may have changed from EV71 to A6 and A10. We can think about modeling from the evolution of the strain in the future, so as to study the impact of different genotypes of enterovirus in different years and seasons, which belong to a multi-strain problem in epidemiological dynamics.

6. Conclusion

This paper aims to study the mechanism of the multi-wave outbreak of HFMD. We set up the dynamical HFMD models, considering time-varying transmission rates with two climate-environmental factors (temperature, relative humidity) and one people's behavior-altering factor (school opening and closing). The relationship between temperature and relative humidity and the infection of HFMD is exponential and quadratic, respectively, obtained by DLNM. This idea makes up for the lack of consideration of the transmission rate function in the HFMD dynamics model. Then, we fit the four models to the data of reported cases in Shanghai from 2012 to 2019. According to the fitted figure and model selection criteria, all three factors are vital for explaining the multi-wave outbreak of HFMD. In addition, the temperature is the most important, followed by school opening and closing and relative humidity, which may provide positive information for the prevention and control of HFMD. However, the $[R_0]$ of Stage I (without vaccine) and Stage II (with EV71 vaccine) are 1.9362 and 1.5478, respectively, which indicates continued transmission of HFMD. The continued spread of HFMD may be due to low vaccination rates against the dominant strain EV71, the dominant strain be replacing, or mutations in the dominant virus that allow HFMD to continue to spread despite the vaccine. Thus, we obtain three conclusions about the prevention and control of HFMD. 1) According to the temperature, relative humidity and school start time, the outbreak peak of HFMD should be warned and targeted prevention and control measures should be taken. 2) Reduce high indoor temperature when more than 31.5 ^{o}C, and increase low relative humidity when less than 77.5% by opening the window for ventilation, adding houseplants, using air conditioners and humidifiers, reducing the incidence of HFMD and the number of infections. 3) The risk of HFMD transmission during winter vacations is higher than during summer vacations. It is necessary to strengthen the publicity of HFMD prevention knowledge before winter vacations and strengthen the disinfection control measures during winter vacations in children's hospitals, school classrooms, and other places where children gather to reduce the frequency of staff turnover during winter vacations.

Finally, although our study may not have much reference significance for regions with different climates, it is worth noting that our method can be applied to other regions. In the future, we will consider more and smaller areas and analyze the outbreak mechanism of minor holidays and Lunar New Year according to the reported daily data, considering the differences in age, gender, and disease strains to make more detailed studies.

Author contribution statement

Changlei Tan: Performed the experiments, Analyzed and interpreted the data, Wrote the paper; **Shuang Li:** Analyzed and interpreted the data; **Yong Li:** Analyzed and interpreted the data, Conceived and designed the experiments; **Zhihang Peng:** Analyzed and interpreted the data, Conceived and designed the experiments.

Data availability statement

The HFMD case data that support this study are available from the Shanghai Municipal Health Commission (https://wsjkw.sh.gov.cn/yqxx/index_2.html). The other data sources are detailed in Section 2.1 of this study. The above network direct data are completely open, and we count these data.

Declaration of competing interest

The authors declare that they have no known competing financial interests or personal relationships that could have appeared to influence the work reported in this paper.

Acknowledgements

This research was supported in part by the National Natural Science Foundation of China (Grant Nos. 11901059, 82073673), the National Key R&D Plan (Grant No. 2022YFC2304000) and the Priority 396 Academic Program Development of Jiangsu Higher Education Institutions (PAPD). The funders had no role in study design, data collection and analysis, decision to publish, or preparation of the manuscript.

Appendix A. The process of calculate $[R_0]$

The next generation matrix method rewrites the system as $\mathscr{F} - \mathscr{V}$, and preserves 4 infected compartments (E, I, I_e, H):

$$\mathscr{F} = (f(t), 0, 0, 0)^T, \tag{A.1}$$

which

$$f(t) = \begin{cases} \frac{\beta(t)(I+I_e)S}{N}, & t \le November\ 2016, \\ \frac{\beta(t)(I+I_e)((1-\rho)+r\rho)S}{N}, & t > November\ 2016, \end{cases} \tag{A.2}$$

and

$$\mathscr{V} = \begin{pmatrix} (\sigma+\mu)E \\ -\sigma pE + (\gamma_1+\mu)I \\ -\sigma(1-p)E + (\gamma_2+\mu)I_e \\ -\gamma_1 qI + (\gamma_3+d+\mu)H \end{pmatrix}. \tag{A.3}$$

The disease-free equilibrium (DFE) of the system is $E_0 = (\frac{\Lambda}{\mu}, 0, 0, 0, 0, 0)$.
Calculating the Jacobian matrices at the DFE, we have,

$$F = \begin{pmatrix} 0 & \frac{\partial f}{\partial I} & \frac{\partial f}{\partial I_e} & 0 \\ 0 & 0 & 0 & 0 \\ 0 & 0 & 0 & 0 \\ 0 & 0 & 0 & 0 \end{pmatrix}, \tag{A.4}$$

which

$$\frac{\partial f}{\partial I} = \frac{\partial f}{\partial I_e} = \begin{cases} \overline{\beta}, & t \le November\ 2016, \\ \overline{\beta}(1-\rho+r\rho), & t > November\ 2016, \end{cases} \tag{A.5}$$

and $\overline{\beta} = \frac{1}{T}\int_0^T \beta(t)dt$, which T shows the epidemic period of HFMD.

$$V = \begin{pmatrix} \sigma+\mu & 0 & 0 & 0 \\ -p\sigma & \gamma_1+\mu & 0 & 0 \\ -(1-p)\sigma & 0 & \gamma_2+mu & 0 \\ 0 & -q\gamma_1 & 0 & \gamma_3+\mu+d \end{pmatrix}, \tag{A.6}$$

$$V^{-1} = \begin{pmatrix} 1/(\sigma+\mu) & 0 & 0 & 0 \\ p\sigma/((\sigma+\mu)(\gamma_1+\mu)) & 1/(\gamma_1+\mu) & 0 & 0 \\ (1-p)\sigma/((\sigma+\mu)(\gamma_2+\mu)) & 0 & 1/(\gamma_2+\mu) & 0 \\ pq\sigma/((\sigma+\mu)(\gamma_1+\mu)(\gamma_3+\mu+d)) & q\gamma_1/((\gamma_1+\mu)(\gamma_3+\mu+d)) & 0 & 1/(\gamma_3+\mu+d) \end{pmatrix}. \tag{A.7}$$

So $[R_0]$ is the maximum spectral radius of (FV^{-1}),

$$[R_0] = \begin{cases} \frac{\overline{\beta}\sigma(p\gamma_2+(1-p)\gamma_1+\mu)}{(\sigma+\mu)(\gamma_1+\mu)(\gamma_2+\mu)}, & t \le November\ 2016, \\ \frac{\overline{\beta}\sigma(p\gamma_2+(1-p)\gamma_1+\mu)(1-\rho+r\rho)}{(\sigma+\mu)(\gamma_1+\mu)(\gamma_2+\mu)}, & t > November\ 2016. \end{cases} \tag{A.8}$$

Appendix B. Supplementary material

Supplementary material related to this article can be found online at https://doi.org/10.1016/j.heliyon.2023.e18212.

References

[1] National Health Commission, PRC, Hand-foot-and-mouth Disease Diagnosis and Treatment Guidelines, (2018 Edition), http://www.weihaicdc.cn/module/download/downfile.jsp?classid=0&filename=1805250922251407696.pdf, 2018.
[2] R. Li, L. Liu, Z. Mo, X. Wang, J. Xia, Z. Liang, Y. Zhang, Y. Li, Q. Mao, J. Wang, et al., An inactivated enterovirus 71 vaccine in healthy children, N. Engl. J. Med. 370 (9) (2014) 829–837.
[3] Centers for Disease Control and Prevention (CDC), Viruses that cause hand, foot, and mouth disease, https://www.cdc.gov/hand-foot-mouth/about/transmission.html, 2021.
[4] World Health Organization (WHO), Enterovirus 71, https://www.who.int/teams/health-product-policy-and-standards/standards-and-specifications/vaccine-standardization/enterovirus-71, 2021.
[5] D. Ventarola, L. Bordone, N. Silverberg, Update on hand-foot-and-mouth disease, Clin. Dermatol. 33 (3) (2015) 340–346.
[6] S. Aswathyraj, G. Arunkumar, E. Alidjinou, D. Hober, Hand, foot and mouth disease (HFMD): emerging epidemiology and the need for a vaccine strategy, Med. Microbiol. Immunol. 205 (5) (2016) 397–407.
[7] Q. Mao, Y. Wang, L. Bian, M. Xu, Z. Liang, EV-A71 vaccine licensure: a first step for multivalent enterovirus vaccine to control HFMD and other severe diseases, Emerging Microbes Infect. 5 (1) (2016) 1–7.
[8] Y. Zhao, D. Zhou, T. Ni, D. Karia, A. Kotecha, X. Wang, Z. Rao, E.Y. Jones, E.E. Fry, J. Ren, et al., Hand-foot-and-mouth disease virus receptor KREMEN1 binds the canyon of Coxsackie Virus A10, Nat. Commun. 11 (1) (2020) 1–8.
[9] Y.-C. Bo, C. Song, J.-F. Wang, X.-W. Li, Using an autologistic regression model to identify spatial risk factors and spatial risk patterns of hand, foot and mouth disease (HFMD) in Mainland China, BMC Public Health 14 (1) (2014) 1–13.
[10] X.-W. Li, X. Ni, S.-Y. Qian, Q. Wang, R.-M. Jiang, W.-B. Xu, Y.-C. Zhang, G.-J. Yu, Q. Chen, Y.-X. Shang, et al., Chinese guidelines for the diagnosis and treatment of hand, foot and mouth disease, (2018 edition) World J. Pediatr. 14 (5) (2018) 437–447.
[11] H. Qi, Y. Li, J. Zhang, Y. Chen, Y. Guo, S. Xiao, J. Hu, W. Wang, W. Zhang, Y. Hu, et al., Quantifying the risk of hand, foot, and mouth disease (HFMD) attributable to meteorological factors in East China: a time series modelling study, Sci. Total Environ. 728 (2020) 138548.
[12] CDC, Hand, foot, and mouth disease (HFMD), https://www.cdc.gov/hand-foot-mouth/index.html, 2021.
[13] Y. Wang, Z. Feng, Y. Yang, S. Self, Y. Gao, I.M. Longini, J. Wakefield, J. Zhang, L. Wang, X. Chen, et al., Hand, foot and mouth disease in China: patterns of spread and transmissibility during 2008–2009, Epidemiology 22 (6) (2011) 781.
[14] J. Zhao, F. Jiang, L. Zhong, J. Sun, J. Ding, Age patterns and transmission characteristics of hand, foot and mouth disease in China, BMC Infect. Dis. 16 (1) (2016) 1–12.
[15] National Institute for Viral Disease Control and Prevention, China CDC, HFMD, clinical manifestations, incubation period, (in Chinese), https://ivdc.chinacdc.cn/jkzt/kpzs/201811/t20181105_196902.htm, 2018.
[16] CDC, Treat hand, foot, and mouth disease, https://www.cdc.gov/hand-foot-mouth/about/treatment.html, 2021.
[17] J. Gui, Z. Liu, T. Zhang, Q. Hua, Z. Jiang, B. Chen, H. Gu, H. Lv, C. Dong, Epidemiological characteristics and spatial-temporal clusters of hand, foot, and mouth disease in Zhejiang Province, China, 2008–2012, PLoS ONE 10 (9) (2015) 0139109.
[18] F. Zhu, W. Xu, J. Xia, Z. Liang, Y. Liu, X. Zhang, X. Tan, L. Wang, Q. Mao, J. Wu, et al., Efficacy, safety, and immunogenicity of an enterovirus 71 vaccine in China, N. Engl. J. Med. 370 (9) (2014) 818–828.
[19] Chinese Center for Disease Control and Prevention (China CDC), Hand, foot and mouth disease prevention and control core information, (in Chinese), https://www.chinacdc.cn/jkzt/crb/bl/szkb/zstd/201803/t20180326_159976.html, 2018.
[20] L. Li, H. Yin, Z. An, Z. Feng, Considerations for developing an immunization strategy with enterovirus 71 vaccine, Vaccine 33 (9) (2015) 1107–1112.
[21] S.Y.-F. Lau, E. Chen, K.N. Mohammad, J. Cai, M.H. Wang, B.C.-Y. Zee, S. Zhao, K.C. Chong, X. Wang, Ambient temperature and relative humidity as possible drivers of the hand, foot, and mouth disease epidemics in Zhejiang Province, China, Atmos. Environ. 244 (2021) 117984.
[22] J. Liu, Threshold dynamics for a HFMD epidemic model with periodic transmission rate, Nonlinear Dyn. 64 (1) (2011) 89–95.
[23] Y. Ma, M. Liu, Q. Hou, J. Zhao, Modelling seasonal HFMD with the recessive infection in Shandong, China, Math. Biosci. Eng. 10 (4) (2013) 1159.
[24] Y. Li, J. Zhang, X. Zhang, Modeling and preventive measures of hand, foot and mouth disease (HFMD) in China, Int. J. Environ. Res. Public Health 11 (3) (2014) 3108–3117.
[25] L. Shi, H. Zhao, D. Wu, Modelling and analysis of HFMD with the effects of vaccination, contaminated environments and quarantine in Mainland China, Math. Biosci. Eng. 16 (1) (2019) 474–500.
[26] Z. Ding, Y. Li, Y. Cai, Y. Dong, W. Wang, Optimal control strategies of HFMD in Wenzhou, China, Complexity 2020 (2020).
[27] S. Takahashi, Q. Liao, T.P. Van Boeckel, W. Xing, J. Sun, V.Y. Hsiao, C.J.E. Metcalf, Z. Chang, F. Liu, J. Zhang, et al., Hand, foot, and mouth disease in China: modeling epidemic dynamics of enterovirus serotypes and implications for vaccination, PLoS Med. 13 (2) (2016) 1001958.
[28] H. Tan, H. Cao, The dynamics and optimal control of a hand-foot-mouth disease model, Comput. Math. Methods Med. 2018 (2018).
[29] L. Shi, H. Zhao, D. Wu, Dynamical analysis for a reaction-diffusion HFMD model with nonsmooth saturation treatment function, Commun. Nonlinear Sci. Numer. Simul. 95 (2021) 105593.
[30] L. Shi, H. Zhao, D. Wu, A reaction-diffusion HFMD model with nonsmooth treatment function, Adv. Differ. Equ. 2021 (1) (2021) 1–19.
[31] S. Majee, S. Jana, D.K. Das, T. Kar, Global dynamics of a fractional-order HFMD model incorporating optimal treatment and stochastic stability, Chaos Solitons Fractals 161 (2022) 112291.
[32] Y. Li, L. Wang, L. Pang, S. Liu, The data fitting and optimal control of a hand, foot and mouth disease (HFMD) model with stage structure, Appl. Math. Comput. 276 (2016) 61–74.
[33] J. Wang, Y. Xiao, R.A. Cheke, Modelling the effects of contaminated environments on HFMD infections in mainland China, Biosystems 140 (2016) 1–7.
[34] J. Wang, Y. Xiao, Z. Peng, Modelling seasonal HFMD infections with the effects of contaminated environments in mainland China, Appl. Math. Comput. 274 (2016) 615–627.
[35] J.-Y. Yang, Y. Chen, F.-Q. Zhang, Stability analysis and optimal control of a hand-foot-mouth disease (HFMD) model, J. Appl. Math. Comput. 41 (1) (2013) 99–117.
[36] Y. Li, M. Huang, L. Peng, A multi-group model for estimating the transmission rate of hand, foot and mouth disease in mainland China, Math. Biosci. Eng. 16 (4) (2019) 2305–2321.
[37] S. Chadsuthi, S. Wichapeng, The modelling of hand, foot, and mouth disease in contaminated environments in Bangkok, Thailand, Comput. Math. Methods Med. 2018 (2018).
[38] P. Poletti, M. Ajelli, S. Merler, The effect of risk perception on the 2009 H1N1 pandemic influenza dynamics, PLoS ONE 6 (2) (2011) 16460.
[39] L. Wessel, Y. Hua, J. Wu, S.M. Moghadas, Public health interventions for epidemics: implications for multiple infection waves, BMC Public Health 11 (1) (2011) 1–9.
[40] D. He, J. Dushoff, T. Day, J. Ma, D.J. Earn, Inferring the causes of the three waves of the 1918 influenza pandemic in England and Wales, Proc. R. Soc. Lond. B, Biol. Sci. 280 (1766) (2013) 20131345.
[41] D. He, J. Dushoff, R. Eftimie, D.J. Earn, Patterns of spread of influenza A in Canada, Proc. R. Soc. Lond. B, Biol. Sci. 280 (1770) (2013) 20131174.
[42] A. Gasparrini, B. Armstrong, M.G. Kenward, Distributed lag non-linear models, Stat. Med. 29 (21) (2010) 2224–2234.
[43] A. Gasparrini, Distributed lag linear and non-linear models in R: the package dlnm, J. Stat. Softw. 43 (8) (2011) 1.

[44] Z. Tian, S. Li, J. Zhang, J.J. Jaakkola, Y. Guo, Ambient temperature and coronary heart disease mortality in Beijing, China: a time series study, Environ. Health 11 (1) (2012) 1–7.
[45] G. Luan, P. Yin, T. Li, L. Wang, M. Zhou, The years of life lost on cardiovascular disease attributable to ambient temperature in China, Sci. Rep. 7 (1) (2017) 1–8.
[46] Y. Ma, J. Zhou, S. Yang, Z. Yu, F. Wang, J. Zhou, Effects of extreme temperatures on hospital emergency room visits for respiratory diseases in Beijing, China, Environ. Sci. Pollut. Res. 26 (3) (2019) 3055–3064.
[47] Y. Zhao, Z. Huang, S. Wang, J. Hu, J. Xiao, X. Li, T. Liu, W. Zeng, L. Guo, Q. Du, et al., Morbidity burden of respiratory diseases attributable to ambient temperature: a case study in a subtropical city in China, Environ. Health 18 (1) (2019) 1–8.
[48] G. Zhu, Y. Zhu, Z. Wang, W. Meng, X. Wang, J. Feng, J. Li, Y. Xiao, F. Shi, S. Wang, The association between ambient temperature and mortality of the coronavirus disease 2019 (Covid-19) in Wuhan, China: a time-series analysis, BMC Public Health 21 (1) (2021) 1–10.
[49] Shanghai Statistical Yearbook 2021, Total Households, Population, Density of Registered Population and Life Expectancy (1978–2020), http://tjj.sh.gov.cn/tjnj/nj21.htm?d1 = 2021tjnjen/E0201.htm, 2021.
[50] Ministry of Health of the Peoples Republic of China, Diagnostic criteria and principle of management for hand foot mouth disease, (in Chinese), http://www.nhc.gov.cn/yzygj/s3593g/201306/6d935c0f43cd4a1fb46f8f71acf8e245.shtml, 2010.
[51] Shanghai Municipal Health Commission, Epidemic information, http://wsjkw.sh.gov.cn/yqxx/index.html, 2022.
[52] Shanghai Statistical Yearbook 2021, Main climate indicators of every month (2020), http://tjj.sh.gov.cn/tjnj/nj21.htm?d1 = 2021tjnjen/E0103.htm, 2022.
[53] National Bureau of Statistics, China statistical yearbook, (in Chinese), http://www.stats.gov.cn/sj/ndsj/2022/indexch.htm, 2022.
[54] Shanghai Municipal Bureau of Ecology and Environment, Ecological and environmental quality – historical data query of the past 3 years, (in Chinese), https://sthj.sh.gov.cn, 2022.
[55] The Data-center of China Public Health Science, Notifiable infectious disease, https://www.phsciencedata.cn/Share/ky_sjml.jsp?id = %27a56cd203-cd11-414d-9efa-d1583b97476f%27, 2023.
[56] WHO, Using climate to predict infectious disease epidemics, https://www.who.int/publications/i/item/using-climate-to-predict-infectious-disease-epidemics, 2005.
[57] L. Zhu, Z. Yuan, X. Wang, J. Li, L. Wang, Y. Liu, F. Xue, Y. Liu, The impact of ambient temperature on childhood HFMD incidence in inland and coastal area: a two-city study in Shandong Province, China, Int. J. Environ. Res. Public Health 12 (8) (2015) 8691–8704.
[58] W. Dong, P. Yang, H. Liao, X. Wang, Q. Wang, et al., The effects of weather factors on hand, foot and mouth disease in Beijing, Sci. Rep. 6 (1) (2016) 1–9.
[59] Shanghai Municipal Education Commission Address, Academic status and academic calendar, (in Chinese), https://edu.sh.gov.cn/xxgk2_zdgz_jcjy_05/index.html, 2022.
[60] China CDC, Technical guide for inactivated enterovirus 71 vaccine, (in Chinese), https://www.chinacdc.cn/zxdt/201606/W020160608725047001222.pdf, 2016.
[61] P. Van den Driessche, J. Watmough, Reproduction numbers and sub-threshold endemic equilibria for compartmental models of disease transmission, Math. Biosci. 180 (1–2) (2002) 29–48.
[62] J. Hao, Z. Yang, W. Yang, S. Huang, L. Tian, Z. Zhu, Y. Lu, H. Xiang, S. Liu, Impact of ambient temperature and relative humidity on the incidence of hand-foot-mouth disease in Wuhan, China, Int. J. Environ. Res. Public Health 17 (2) (2020) 428.
[63] C. Chen, Q. Jiang, Z. Song, Y. Li, H. Wang, Y. Lu, D. Wang, M. Li, T. Li, Influence of temperature and humidity on hand, foot, and mouth disease in Guangzhou, 2013–2017, J. Int. Med. Res. 48 (6) (2020) 0300060520929895.
[64] C. Fan, F. Liu, X. Zhao, Y. Ma, F. Yang, Z. Chang, X. Xiao, An alternative comprehensive index to quantify the interactive effect of temperature and relative humidity on hand, foot and mouth disease: a two-stage time series study including 143 cities in mainland China, Sci. Total Environ. 740 (2020) 140106.
[65] Q. Zhao, S. Li, W. Cao, D.-L. Liu, Q. Qian, H. Ren, F. Ding, G. Williams, R. Huxley, W. Zhang, et al., Modeling the present and future incidence of pediatric hand, foot, and mouth disease associated with ambient temperature in mainland China, Environ. Health Perspect. 126 (4) (2018) 047010.
[66] Q. Wei, J. Wu, Y. Zhang, Q. Cheng, L. Bai, J. Duan, J. Gao, Z. Xu, W. Yi, R. Pan, et al., Short-term exposure to sulfur dioxide and the risk of childhood hand, foot, and mouth disease during different seasons in Hefei, China, Sci. Total Environ. 658 (2019) 116–121.
[67] G. Yu, Y. Li, J. Cai, D. Yu, J. Tang, W. Zhai, Y. Wei, S. Chen, Q. Chen, J. Qin, Short-term effects of meteorological factors and air pollution on childhood hand-foot-mouth disease in Guilin, China, Sci. Total Environ. 646 (2019) 460–470.
[68] F. Yin, T. Zhang, L. Liu, Q. Lv, X. Li, The association between ambient temperature and childhood hand, foot and mouth disease in Chengdu, China: a distributed lag non-linear analysis, Sci. Rep. 6 (1) (2016) 1–9.
[69] F. Yin, Y. Ma, X. Zhao, Q. Lv, Y. Liu, X. Li, T. Zhang, Analysis of the effect of PM10 on hand, foot and mouth disease in a basin terrain city, Sci. Rep. 9 (1) (2019) 1–6.
[70] H. Qi, Y. Chen, D. Xu, H. Su, L. Zhan, Z. Xu, Y. Huang, Q. He, Y. Hu, H. Lynn, et al., Impact of meteorological factors on the incidence of childhood hand, foot, and mouth disease (HFMD) analyzed by DLNMs-based time series approach, Infect. Dis. Poverty 7 (1) (2018) 1–10.
[71] Y.L. Hii, J. Rocklöv, N. Ng, Short term effects of weather on hand, foot and mouth disease, PLoS ONE 6 (2) (2011) 16796.
[72] X. Xiao, A. Gasparrini, J. Huang, Q. Liao, F. Liu, F. Yin, H. Yu, X. Li, The exposure-response relationship between temperature and childhood hand, foot and mouth disease: a multicity study from mainland China, Environ. Int. 100 (2017) 102–109.
[73] J.M. Ver Hoef, P.L. Boveng, Quasi-Poisson vs. negative binomial regression: how should we model overdispersed count data?, Ecology 88 (11) (2007) 2766–2772.
[74] A.C. Davison, D.V. Hinkley, Bootstrap Methods and Their Application, vol. 1, 1997.
[75] T. Hesterberg, Bootstrap, Wiley Interdiscip. Rev.: Comput. Stat. 3 (6) (2011) 497–526.
[76] National Bureau of Statistics, Shanghai 6th National Population Census 2010 Main Data Bulletin. Fourth, age composition, (in Chinese), http://www.stats.gov.cn/tjsj/tjgb/rkpcgb/dfrkpcgb/201202/t20120228_30403.html, 2021.
[77] Shanghai Statistical Yearbook 2021, Birth rate, death rate and natural growth rate of population in main years, http://tjj.sh.gov.cn/tjnj/nj21.htm?d1 = 2021tjnjen/E0203.htm, 2021.
[78] J. Li, Y. Wei, B. Dong, M. Chen, M. Chen, H. Li, Y. Su, R. Li, Trends of morbidity and mortality of hand foot and mouth disease in China, 2008–2017, Dis. Surveill. 37 (2) (2022) 233–240.
[79] National Health Commission, PRC, Statistical Bulletin on China's Health Development 2019, (in Chinese), http://www.nhc.gov.cn/guihuaxxs/s10748/202006/ebfe31f24cc145b198dd730603ec4442.shtml, 2020.
[80] X. Zhang, Y. Zhao, A.U. Neumann, Partial immunity and vaccination for influenza, J. Comput. Biol. 17 (12) (2010) 1689–1696.
[81] Y. Li, L.-W. Wang, Z.-H. Peng, H.-B. Shen, Basic reproduction number and predicted trends of coronavirus disease 2019 epidemic in the mainland of China, Infect. Dis. Poverty 9 (1) (2020) 1–13.
[82] Y. Li, X. Liu, Y. Yuan, J. Li, L. Wang, Global analysis of tuberculosis dynamical model and optimal control strategies based on case data in the United States, Appl. Math. Comput. 422 (2022) 126983.
[83] M.R. Sierra, C.A. Coello Coello, Improving PSO-based multi-objective optimization using crowding, mutation and dominance, in: International Conference on Evolutionary Multi-Criterion Optimization, Springer, 2005, pp. 505–519.
[84] C.-L. Huang, J.-F. Dun, A distributed PSO–SVM hybrid system with feature selection and parameter optimization, Appl. Soft Comput. 8 (4) (2008) 1381–1391.
[85] F. Marini, B. Walczak, Particle swarm optimization (PSO). A tutorial, Chemom. Intell. Lab. Syst. 149 (2015) 153–165.
[86] H. Miao, C. Dykes, L.M. Demeter, H. Wu, Differential equation modeling of HIV viral fitness experiments: model identification, model selection, and multimodel inference, Biometrics 65 (1) (2009) 292–300.

[87] G. Schwarz, Estimating the dimension of a model, Ann. Stat. (1978) 461–464.
[88] D. Anderson, K. Burnham, G. White, Comparison of Akaike information criterion and consistent Akaike information criterion for model selection and statistical inference from capture-recapture studies, J. Appl. Stat. 25 (2) (1998) 263–282.
[89] Y. Miche, A. Lendasse, A faster model selection criterion for OP-ELM and OP-KNN: Hannan-Quinn criterion, in: ESANN, vol. 9, 2009, pp. 177–182.
[90] D. Greenhalgh, I. Moneim, SIRS epidemic model and simulations using different types of seasonal contact rate, Syst. Anal. Model. Simul. 43 (5) (2003) 573–600.
[91] J. Ma, Z. Ma, Epidemic threshold conditions for seasonally forced SEIR models, Math. Biosci. Eng. 3 (1) (2006) 161.
[92] W. Wang, X.-Q. Zhao, Threshold dynamics for compartmental epidemic models in periodic environments, J. Dyn. Differ. Equ. 20 (3) (2008) 699–717.
[93] Z. Bo, Y. Ma, Z. Chang, T. Zhang, F. Liu, X. Zhao, L. Long, X. Yi, X. Xiao, Z. Li, The spatial heterogeneity of the associations between relative humidity and pediatric hand, foot and mouth disease: evidence from a nation-wide multicity study from mainland China, Sci. Total Environ. 707 (2020) 136103.